NASA TECHNICAL NOTE

NASA TN D-6523

a.1

NASA TN D-6523

LOAN COPY: RETURN
AFWL (DOUL)
KIRTLAND AFB, N. M

TECH LIBRARY KAFB, NM

0133743

EXPERIMENTAL INVESTIGATION OF LAMINAR GAS JET DIFFUSION FLAMES IN ZERO GRAVITY

by Thomas H. Cochran

Lewis Research Center

Cleveland, Ohio 44135

NATIONAL AERONAUTICS AND SPACE ADMINISTRATION • WASHINGTON, D. C. • JANUARY 1972

TECH LIBRARY KAFB, NM

0133413

1. Report No. NASA TN D-6523	2. Government Accession No.	3. Recipie...
4. Title and Subtitle EXPERIMENTAL INVESTIGATION OF LAMINAR GAS JET DIFFUSION FLAMES IN ZERO GRAVITY		5. Report Date January 1972
		6. Performing Organization Code
7. Author(s) Thomas H. Cochran		8. Performing Organization Report No. E-6570
		10. Work Unit No. 111-05
9. Performing Organization Name and Address Lewis Research Center National Aeronautics and Space Administration Cleveland, Ohio 44135		11. Contract or Grant No.
		13. Type of Report and Period Covered Technical Note
12. Sponsoring Agency Name and Address National Aeronautics and Space Administration Washington, D.C. 20546		14. Sponsoring Agency Code
15. Supplementary Notes		

16. Abstract

An experimental program was conducted to study the burning of laminar gas jet diffusion flames in a zero-gravity environment. The tests were conducted in the Lewis Research Center's 2.2-Second-Zero-Gravity Facility and were a part of a continuing effort investigating the effects of gravity on basic combustion processes. The photographic results indicate that steady state gas jet diffusion flames existed in zero gravity but they were geometrically quite different than their normal-gravity counterparts. Methane-air flames were found to be approximately 50 percent longer and wider in zero gravity than in normal gravity.

17. Key Words (Suggested by Author(s)) Diffusion flames Zero gravity Spacecraft safety	18. Distribution Statement Unclassified - unlimited		
19. Security Classif. (of this report) Unclassified	20. Security Classif. (of this page) Unclassified	21. No. of Pages 28	22. Price* $3.00

* For sale by the National Technical Information Service, Springfield, Virginia 22151

EXPERIMENTAL INVESTIGATION OF LAMINAR GAS JET DIFFUSION FLAMES IN ZERO GRAVITY

by Thomas H. Cochran
Lewis Research Center

SUMMARY

An experimental program was conducted to study the burning of laminar gas jet diffusion flames in a zero-gravity environment. The tests were conducted in the Lewis Research Center's 2.2-Second Zero-Gravity Facility and were a part of a continuing effort investigating the effects of gravity on basic combustion processes. The photographic results indicate that steady state gas jet diffusion flames existed in zero gravity but they were geometrically quite different than their normal gravity counterparts. Methane-air flames were found to be approximately 50 percent longer and wider in zero gravity than in normal gravity.

INTRODUCTION

The various processes incorporated under the general heading of burning have been the subject of numerous scientific investigations. The myriad of practical applications of combustion processes easily justify such studies. In terms of their effect on man, these processes may be categorized as either beneficial, such as controlled combustion in a jet engine, or hazardous, as exemplified by a destructive fire. A particular problem in the latter category, fires aboard spacecraft, has prompted this report.

The type of combustion process expected, should a fire occur in space, is termed a diffusion flame. Diffusion flames are characterized by the fact that the rate of mixing of the fuel and oxidant, a fluid dynamic process, rather than the rate of chemical reaction controls the combustion process. Therefore, since temperatures in flames are characteristically high ($\approx 2000^{\circ}$ C), buoyancy, or the lack of it, may affect the flame.

Since the onset of space travel, an increasing number of investigators have focused their attention on the effects of gravity on combustion processes. A review of the experimental work on this subject is contained in reference 1. Recent publications include an analytical study of laminar free-convective burning of fuel surfaces (ref. 2), an updating of past work on the burning of liquid droplets in zero gravity (ref. 3), a study of radiative extinguishment of diffusion flames at zero gravity (ref. 4), an investigation of butyl alcohol burning in a channel in zero gravity (ref. 5), and an experimental study of teflon-insulated wires burning in supercritical oxygen in normal and zero gravities (ref. 6).

This report presents the results of research conducted in the Lewis Research Center's 2.2-Second Zero-Gravity Facility on the effects of gravity on laminar gas jet diffusion flames. It is an extension of work reported in references 1 and 7. Color motion pictures were taken of methane burning in air in normal and zero gravity. Fuel flow rates at the burner ranged from 0.75 to 12.20 cubic centimeters per second for burners 0.051, 0.0825, and 0.113 centimeter in radius. The Reynolds number based on the fuel exiting from the burner ranged from approximately 18 to 250.

SYMBOLS

Gr	Grashof number, $(\rho_M^2 \Delta T_{AF} \beta_M g R_o^3)/\mu_M^2$
g	acceleration due to gravity, cm/sec^2
L	flame length, cm
L_s	steady state zero-gravity flame length, cm
L_0	zero-gravity minimum flame length, cm
L_1	normal-gravity flame length, cm
Re	Reynolds number, $(\rho U_\infty R_o)/\mu$
R_{max}	maximum flame radius, cm
R_o	burner radius, cm
T_{AF}	adiabatic flame temperature, $^{\circ}C$
ΔT_{AF}	$T_{AF} - T_{AM}$, $^{\circ}C$
T_{AM}	ambient air temperature, $^{\circ}C$
U_∞	average axial fuel velocity at burner, cm/sec
β	coefficient of thermal expansion, $^{\circ}C^{-1}$
ρ	density, g/cm^3
μ	dynamic viscosity, g/(cm)(sec)

Subscripts:

A air

F fuel

M mean temperature condition

0G zero gravity

1G normal gravity

APPARATUS AND PROCEDURE

The experimental investigation was conducted in the Lewis Research Center's 2.2-Second Zero-Gravity Facility. A complete description of this facility, the experiment package, and the test procedure can be found in the appendix.

The flames were generated by igniting fuel which flowed out of a tube into a quiescent atmosphere of air which was at standard temperature and pressure. The tube was oriented in an upright position as shown in the schematic diagram in figure 1. The tube was long enough and the flow rates low enough so that the fuel flow could be considered to be fully developed and laminar.

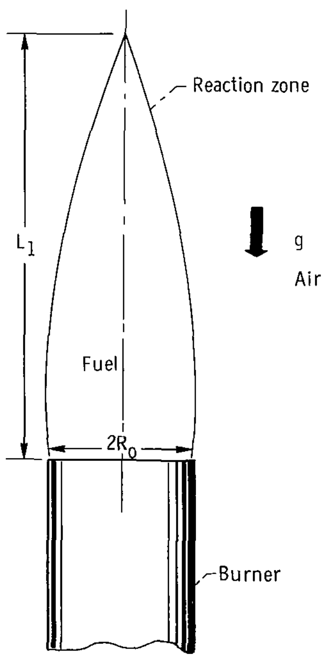

Figure 1. - Normal-gravity laminar gas jet diffusion flame.

DATA REDUCTION

The behavior of the flames was recorded on high-speed, color, 16-millimeter film. A motion analyzer was used to obtain data from this film. In addition to generally observing the phenomena, measurements of flame length as a function of time were made. Scale factors were obtained by photographing scales that extended from the burner to above the heights anticipated for the flames.

RESULTS AND DISCUSSION

Normal-Gravity Calibration

The relation between flame length and flow rate for the different burners was established by conducting tests in normal gravity. The procedure for these tests is detailed in the appendix. It was generally found that the flames under consideration pulsated or oscillated axially on the burner. The magnitude of these oscillations was as much as ±28 percent of the mean length for some of the larger flames. Therefore, an average flame length was defined as the mean of the maximum and minimum lengths.

The data is presented in figure 2 as average flame length as a function of flow rate. Results are shown for the three burners of interest together with the data from reference 1. The latter also investigated methane burning in air; however, the burner sizes were larger than those used in the present tests. Considering the current data first, it can be seen in figure 2 that, for a given burner size, the relationship between flame length and flow rate was approximately linear. Also, for a given flow rate longer flames were obtained as the burner radius became smaller. These results are in contrast to those presented in reference 1 in which no clear effect of burner size on flame length was evident. In other words, for methane-air flames on relatively large burners the flame lengths appeared to be independent of the burner size while for smaller burners the flame lengths were dependent on the size of the burner. These results are similar to those found in reference 8 for city gas flames in air.

Zero-Gravity Data

Observations. - The initial behavior of the flames on entering zero gravity was the same as that described in reference 1. The flames immediately decreased in length after which they expanded away from the burner. As time continued, most of the flames either attained a new steady state condition or extinguished. However, a few were transient, continuously changing during the test time. Photographs of the three types of flames

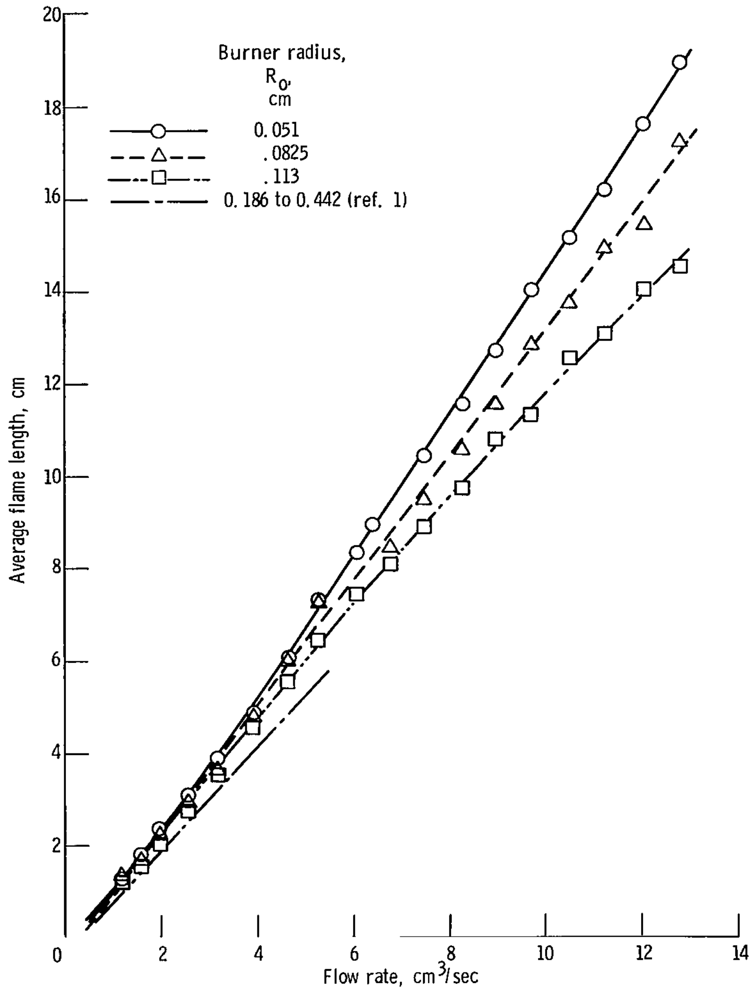

Figure 2. - Average flame length in normal gravity.

(extinguished, transient, and steady state) as a function of time in zero gravity are presented in figures 3, 4, and 5. Figure 3 is taken from reference 1.

A detailed description of flames which extinguish when placed in a zero-gravity environment can be found in references 1 and 7 and, therefore, will not be elaborated upon any further in this report. The transient flames, for the most part, were flames which did not reach a steady length in the time available. There were a few, however, which did reach a new steady length in zero gravity but whose color was changing. The particular transient flame shown in figure 4 was one in which the visible radiation over portions of the flame disappeared (fig. 4(d)) only to reappear at a later time (fig. 4(f)). This could indicate that parts of the flame extinguished and then reignited. Behavior such as this suggests that the transient nature of the fluid dynamics caused by the sudden removal of buoyancy could be contributing to the extinguishment of the flames.

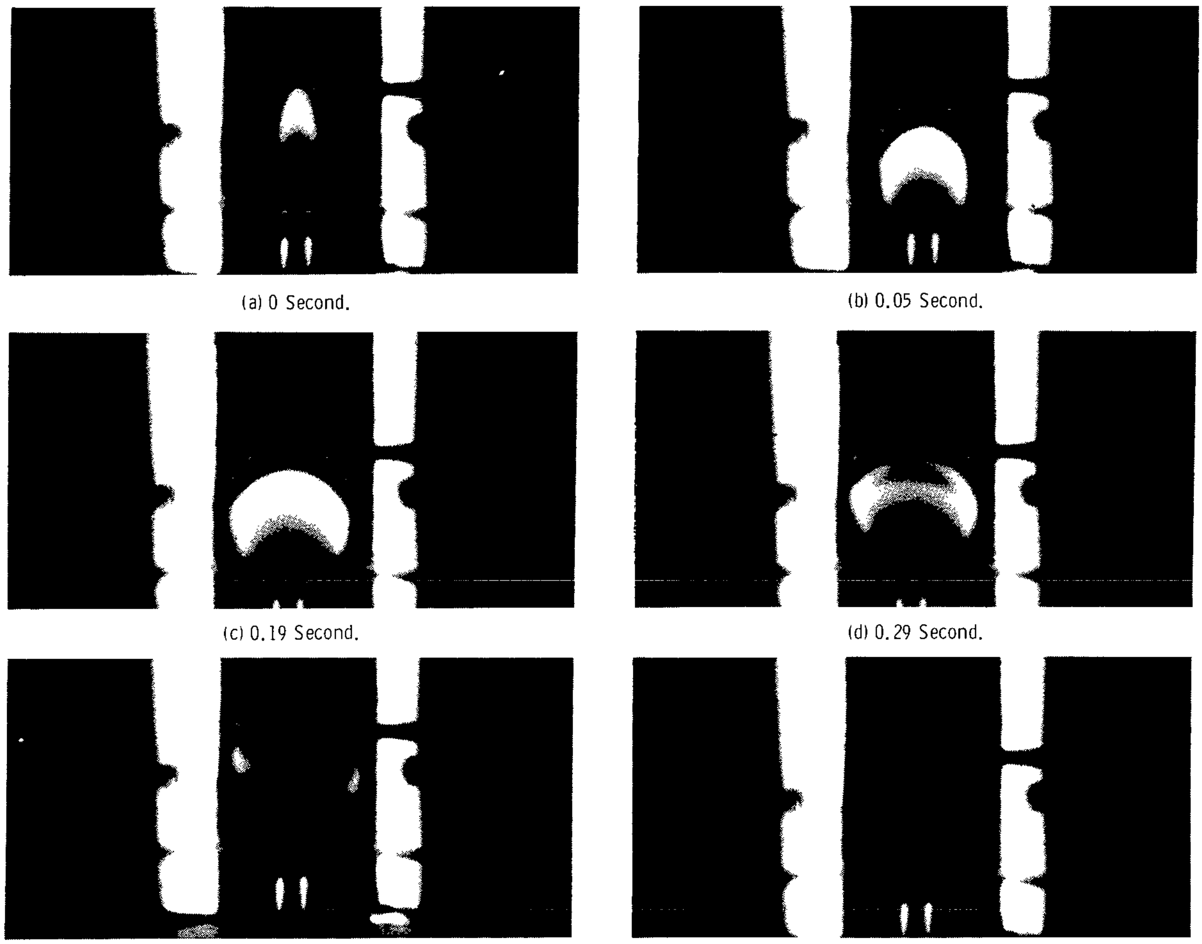

(a) 0 Second. (b) 0.05 Second.

(c) 0.19 Second. (d) 0.29 Second.

(e) 0.55 Second. (f) 0.71 Second.

Time in zero gravity.

Figure 3. - Extinguished zero-gravity gas jet diffusion flame. Run 3 (from ref. 1).

The flames which reached steady state at zero gravity existed in a different shape than they had in normal gravity, as shown by figure 5. The flames were longer and wider in zero gravity than in normal gravity. Also, there was more carbon particle radiation given off by the zero gravity flames. Another significant difference between the normal- and zero-gravity steady state flames was their color, particularly for the larger flames. In normal gravity, the flames were yellow near the top and blue near the burner. However, in zero gravity no blue was present at all. Yellow was apparent in some of the zero-gravity flames toward their center, but, in the main, these flames were orange. A

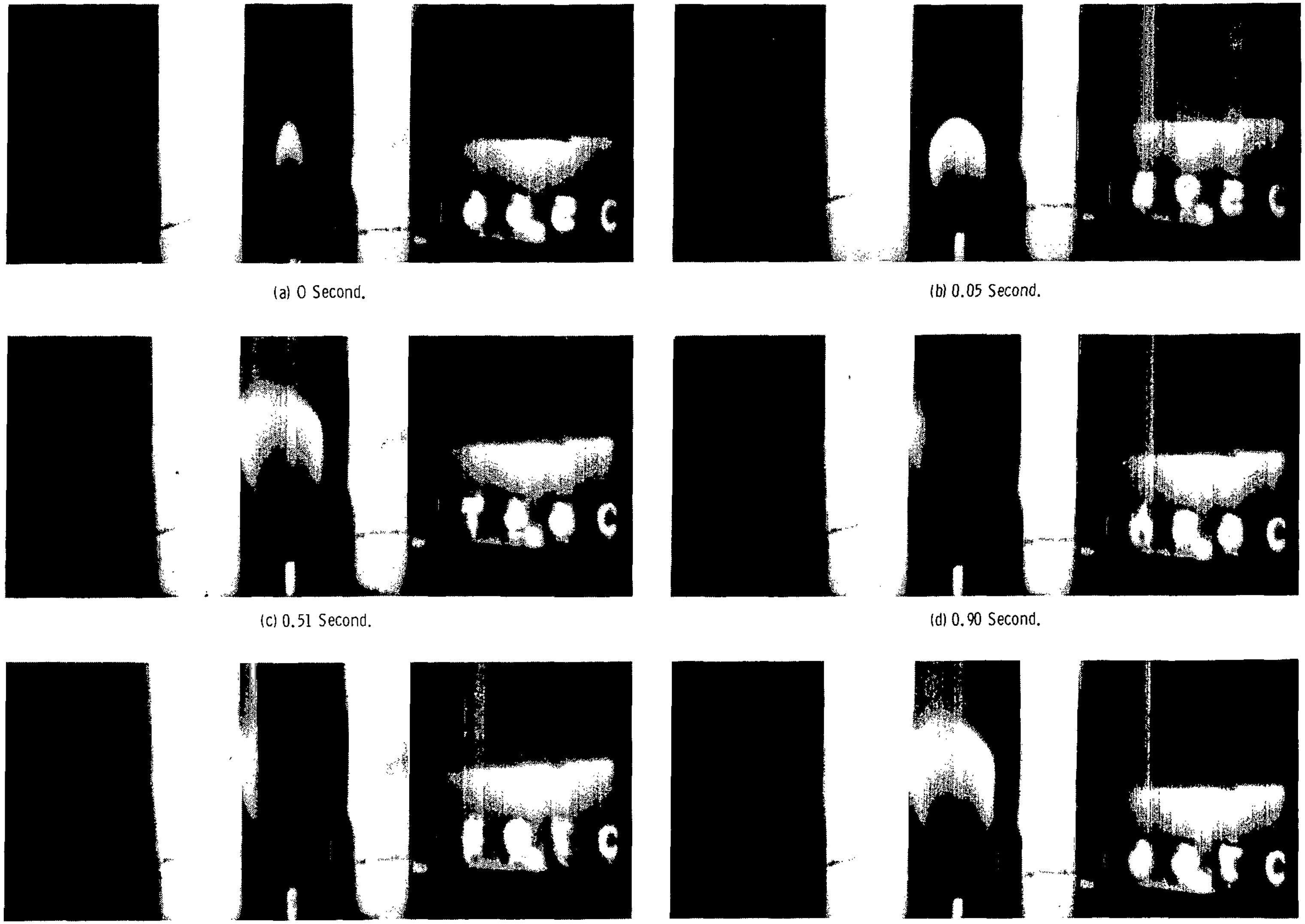

(a) 0 Second.

(b) 0.05 Second.

(c) 0.51 Second.

(d) 0.90 Second.

(e) 1.13 Seconds.

(f) 1.76 Seconds.

Time in zero gravity.

Figure 4. - Transient zero-gravity gas jet diffusion flame. Run 27.

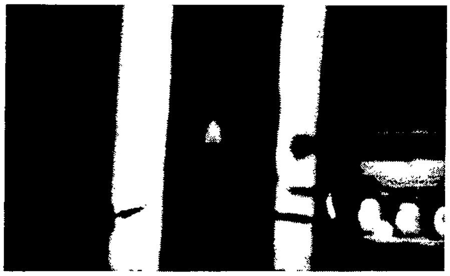

(a) 0 Second.

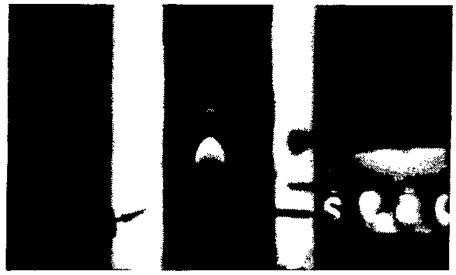

(b) 0.05 Second.

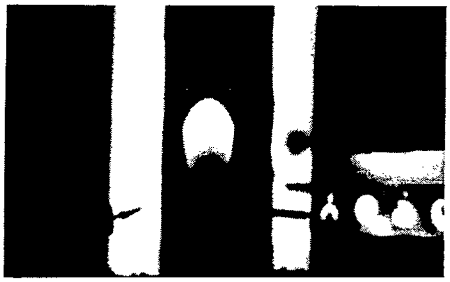

(c) 0.13 Second.

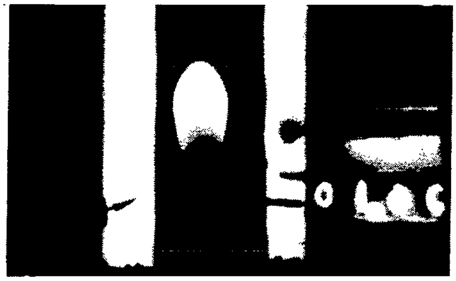

(d) 0.23 Second.

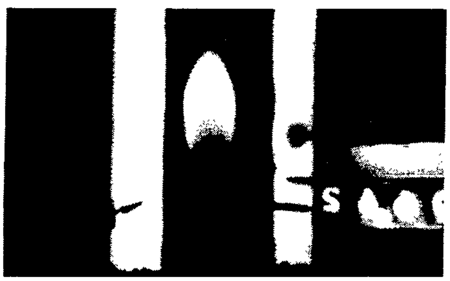

(e) 0.55 Second.

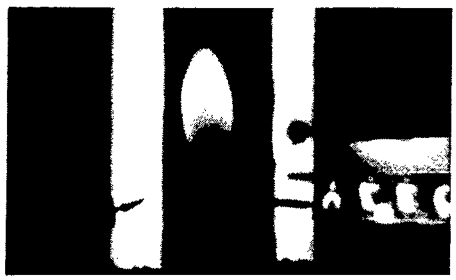

(f) 1.83 Seconds.

Time in zero gravity.

Figure 5. - Steady state zero-gravity gas jet diffusion flame. Run 3.

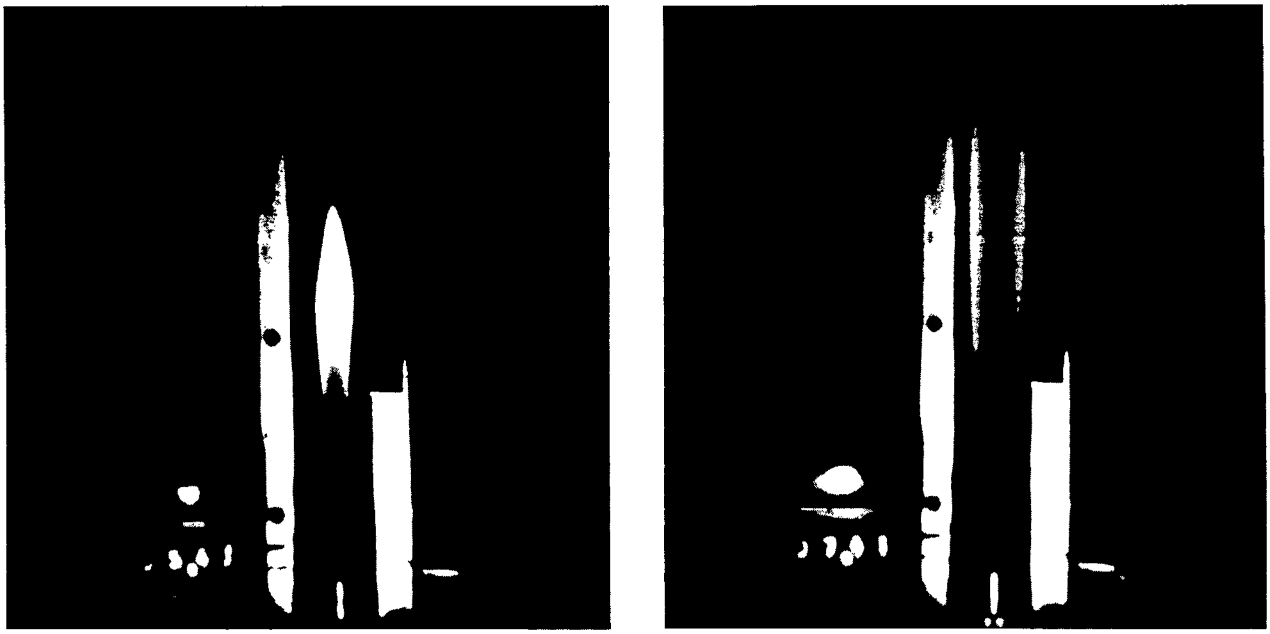

(a) Normal gravity. (b) Zero gravity.

Figure 6. - Steady state flames in normal and zero gravity.

flame which exhibited these color changes is shown in figure 6. If color is taken as a criteria for temperature in the flames, it would appear that some steady state zero-gravity flames are cooler than their counterparts in normal gravity. Also, the tops of some of the steady state zero-gravity flames were very faint (see fig. 6) in contrast to the normal gravity flames which were all very distinct.

As was mentioned previously, a particular characteristic of the flames in normal gravity was that they pulsated. This behavior has been investigated by Toong, Salant, and Stopford in reference 9. These authors attributed the oscillations to the instability of Tollmien-Schlichting disturbance waves - the same mechanism which leads to the onset of transition from laminar to turbulent flow in a boundary layer. The contention is that, when the local Reynolds number in the flow exceeds some critical value, the instabilities occur. In viewing the steady state zero-gravity flames, it was of particular interest that oscillations were all but eliminated. The maximum pulsation was ±1.1 percent of the mean length. This result can be explained by Toong's theory. Since the local velocity over major portions of the flame is reduced in zero gravity as compared to normal gravity because of the absence of buoyancy, the local Reynolds number may be reduced below the critical value necessary for oscillations. Hence, the flames are more stable.

Quantitative data. - Measurements of flame length as a function of time were made for all the test runs. A typical curve of length as a function of time in zero gravity is shown in figure 7. As can be seen, the flame oscillated to some degree in normal grav-

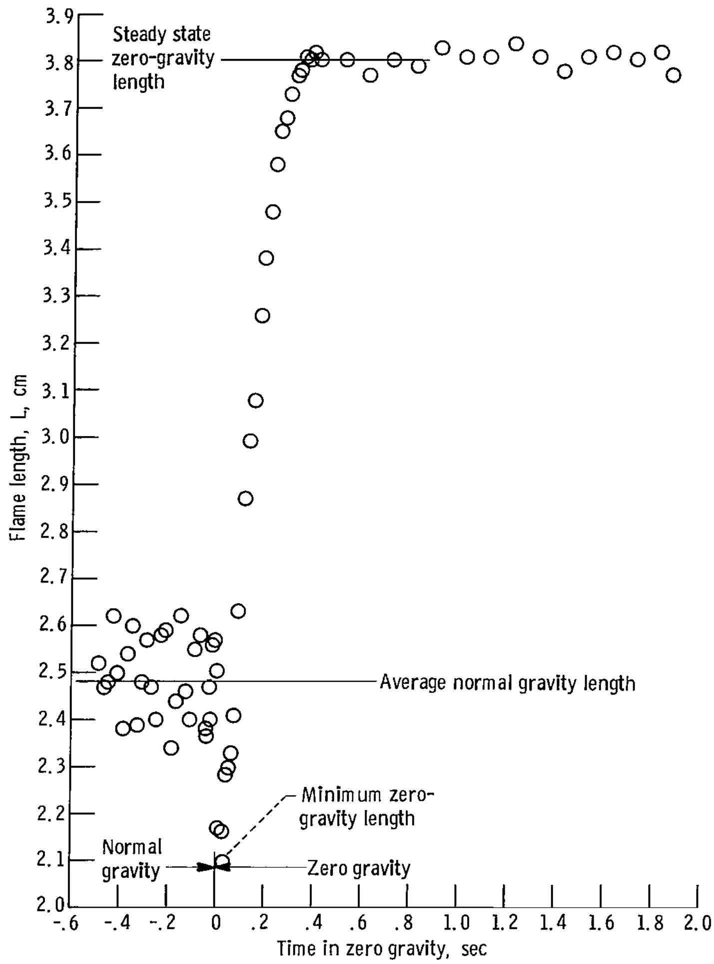

Figure 7. - Flame length as a function of time in zero gravity for run 3.

ity. Upon entering zero gravity, the flame immediately decreased to a minimum zero-gravity length. Subsequently, the flame expanded away from the burner until it reached a new average steady state length. For such steady state flames, the average normal-gravity length, minimum zero-gravity length, and steady state zero-gravity length were recorded. In the case of flames that extinguished, the length at extinguishment was noted in lieu of the steady state zero-gravity length. Finally, for transient flames the only lengths tabulated were the average normal-gravity length and minimum zero-gravity length. The maximum radius was measured for all the flames in normal gravity and for those which reached steady state in zero gravity. These results have been compiled in table I. The flow rate shown in this table was determined from the average normal-gravity length and the length-flow rate curves of figure 2.

Extinguishment length was successfully correlated in reference 1 by nondimensionalizing the data with respect to the radius of the burner and plotting the results as a func-

TABLE I. - TEST DATA

Run	Burner radius, R_o, cm	Average normal-gravity length, L_1, cm	Maximum normal-gravity radius, $R_{max_{1G}}$, cm	Flow rate, cm^3 sec	Average axial velocity, U_∞, cm sec	Zero-gravity minimum length, L_0, cm	Extinguishment length, cm	Steady state zero-gravity length, L_s, cm	Steady state zero-gravity maximum radius, $R_{max_{0G}}$, cm
1	0.051	9.30	0.46	6.65	813.8	7.51	----	(a)	0.77
2		3.42	.37	2.80	342.6	2.96	----	5.02	.70
3		2.48	.37	2.10	291.2	2.10	----	3.80	.72
4		6.95	.51	5.15	630.2	5.91	----	9.78	.83
5		3.51	.42	2.90	354.9	3.08	----	5.38	.74
6		6.54	.51	4.90	599.6	5.59	----	9.76	.78
7		.72	.24	.75	91.8	.68	0.88	-----	----
8		1.08	.32	1.08	132.2	1.04	----	1.80	.48
9		1.76	.44	1.60	195.8	1.63	----	2.76	.60
10	.113	.94	.35	.94	23.4	.78	1.10	-----	----
11		1.88	.40	1.70	42.4	1.46	2.15	-----	----
12		2.22	.41	1.98	49.2	1.60	(b)	-----	----
13		1.08	.36	1.08	26.9	1.01	1.24	-----	----
14		1.22	.33	1.18	29.3	1.01	1.36	-----	----
15		1.92	.38	1.72	42.9	1.48	2.12	-----	----
16		2.46	.38	2.16	53.8	1.81	2.61	-----	----
17		5.92	.55	4.95	123.4	4.50	(b)	-----	----
18		4.20	.51	3.55	88.5	2.65	4.66	-----	----
19		5.13	.58	4.30	107.3	3.36	5.78	-----	----
20		5.80	.60	4.85	120.9	3.76	7.55	-----	----
21		11.43	.69	9.65	240.5	8.91	(b)	-----	----
22		14.13	.73	12.20	304.1	8.96	(a)	-----	----
23	.0825	11.20	.63	8.55	399.8	8.17	----	16.62	.91
24		8.31	.58	6.42	300.2	7.20	----	12.70	.95
25		5.78	.58	4.55	212.9	3.68	----	8.97	1.04
26		3.52	.36	2.90	135.6	2.51	(b)	-----	----
27		2.31	.34	2.00	93.5	1.81	(b)	-----	----
28		.95	.31	1.00	46.8	.82	1.22	-----	----
29		1.65	.35	1.50	70.2	1.42	(b)	-----	----
30		7.06	.48	5.50	257.2	5.21	----	10.86	.92

[a]Out of camera field of view.
[b]Transient flame.

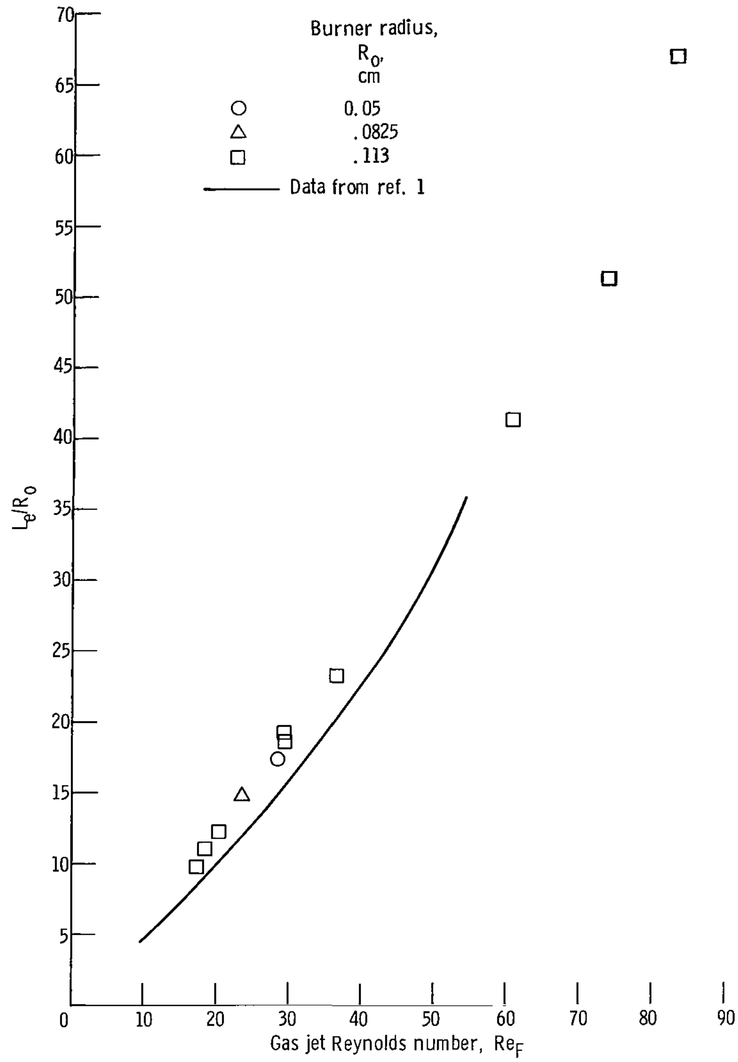

Figure 8. - Dimensionless extinguishment length as a function of gas jet Reynolds number.

tion of gas jet Reynolds number. Figure 8 shows the present data together with the curve from reference 1. It is apparent that there is good agreement between the correlation of reference 1 and the present data.

Steady state flame length for both normal and zero gravity was also nondimensionalized with respect to the particular burner radius. The results are plotted as a function of gas jet Reynolds number in figure 9. It can be seen that the approximately linear relationship evidenced in the normal-gravity data is also reflected in the zero-gravity

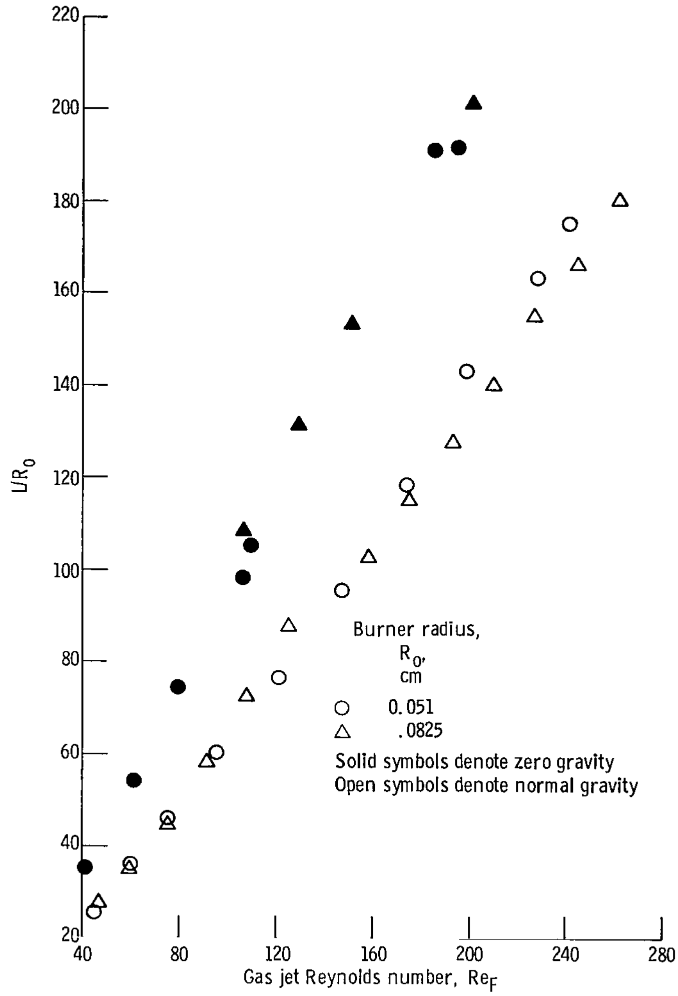

Figure 9. - Dimensionless steady state flame length as a function of gas jet Reynolds number.

data. In addition, figure 9 indicates that steady state zero-gravity flames were approximately 50 percent longer than normal-gravity flames at the same Reynolds number or flow rate. These results are of particular interest when compared to the work of Kimura and Ukawa (ref. 10). In this work, the flame was situated in a duct in which air flowed at controllable rates. The authors investigated both upright and inverted flames. Their results showed that, if fuel and air flowed at the same velocity, the lengths of the normal and inverted flames were the same. However, if the velocity of the air was less than that of the fuel, the normal flame was shorter than the inverted flame. The conclusion of the authors was that buoyancy shortens a flame situated in an upright position in normal gravity, as has been shown by the data herein.

The maximum radius of steady state flames in normal and zero gravity was plotted as a function of flow rate and is presented in figure 10. In general, both normal- and zero-gravity flames became wider as flow rate increased. Also, there is no clear effect

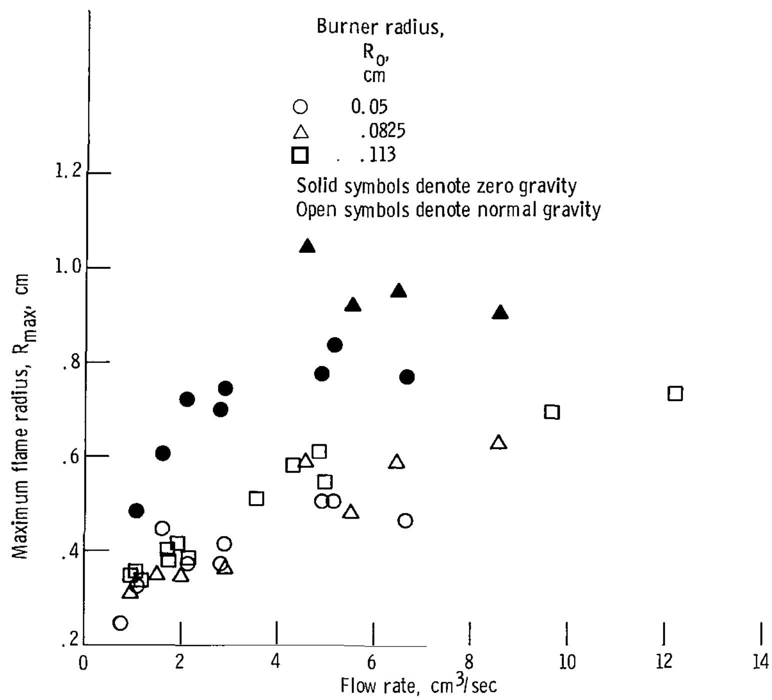

Figure 10. - Effect of gravity on maximum flame radius.

of burner size apparent in the data. A comparison of the normal- and zero-gravity data indicates that the zero-gravity flames were approximately 50 percent wider than normal gravity flames at a particular flow rate.

In reference 1, the fractional decrease in the length of a flame when it is suddenly placed in a zero-gravity environment was selected as a measure of the importance gravity played in the aerodynamics of normal-gravity jet diffusion flames. The fractional decrease was defined as $(L_1 - L_0)/L_1$ where L_1 was the normal-gravity length and L_0 was the minimum zero-gravity length. A dimensional analysis indicated that the parameters descriptive of a normal-gravity flame for a particular fuel were the Reynolds and Grashof numbers. Since it was believed that the primary effect of buoyancy in driving the fluid would be realized on the oxidant side of the reaction zone, the fluid properties used in these parameters were those for air. The characteristic velocity used was the average axial fuel velocity at the burner. The data of reference 1 was correlated using least squares method to obtain the following relation:

$$\frac{L_1 - L_0}{L_1} = 0.09 \left(Gr^{0.37} Re^{0.69}\right)_A$$

This correlating curve together with the data from the present work is shown in figure 11. The agreement between prediction and data is not very satisfying at first glance. The

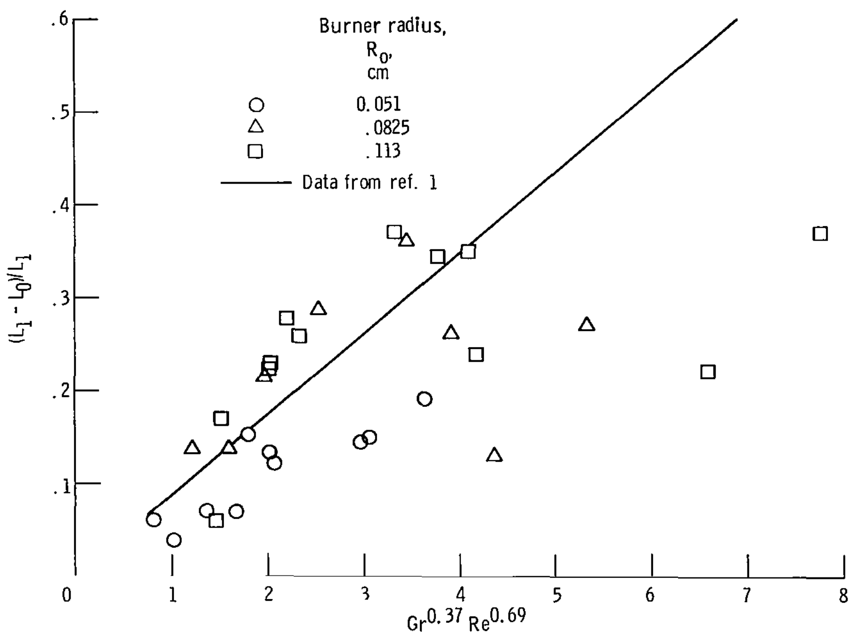

Figure 11. - Effects of gravity-induced momentum on flame length.

discrepancy between predicted and actual values of the fractional decrease is as much as 55 percent in some cases. However, a better measure of the prediction and the data is the difference between the predicted and measured values of the zero-gravity minimum length. This is due to the fact that a small percentage change in the minimum zero-gravity length results in a larger percentage change in the fractional decrease for small values of $L_1 - L_0$. Figure 12 presents the percent difference between the predicted and measured values of the zero-gravity minimum length plotted as a function of flow rate. At lower flow rate, the discrepancy between predicted and measured values is relatively

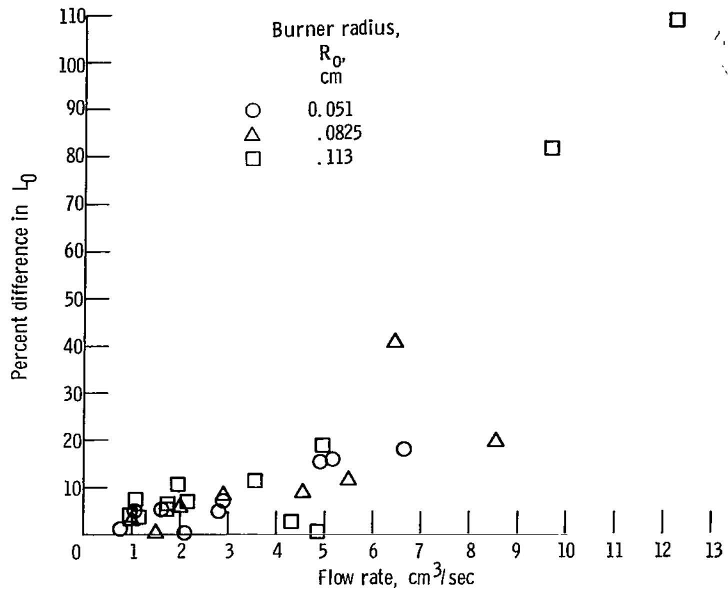

Figure 12. - Percent difference between predicted and measured values of zero-gravity minimum length L_0 as a function of flow rate.

small and can possibly be accounted for by errors in measurement. (Recall that the flow rate was obtained from the average length of a pulsating flame). However, as flow rate increases the predicted and measured values of L_0 deviate too much to be accounted for by such errors. In summary, the correlation of figure 11 is acceptable for lower flow rates. However, the applicability of the correlation at higher flow rates, greater than 6 cubic centimeters per second for these tests, appears tenuous.

Steady state flame geometry in normal and zero gravity. - The most outstanding observed difference between the normal- and zero-gravity steady state flames was, of course, geometrical. Although the differences in flame length or width are convenient to measure and discuss, the overall changes in geometry may be of more value in determining the mechanisms that control the combustion processes. Therefore, the steady state flame profiles in both normal and zero gravity were carefully traced from the motion picture films. The eleven tests for which flames existed in zero gravity are presented in figure 13. For the normal gravity flames, two profiles are generally presented. These are the maximum and minimum shapes of the oscillating flames. Double profiles were not measured for the zero-gravity flames because of their minimal oscillation. In all but two of the flames, the outlines were determined solely by the yellow and orange visible radiation. However, for runs 8 and 9, the photographs were clear enough to use the blue coloration near the burners as a criteria for the boundary of the normal gravity flames. For these profiles, the yellow portions of the flames near their tops are also outlined. The tops of those zero-gravity flames which were faint are represented by dashed lines.

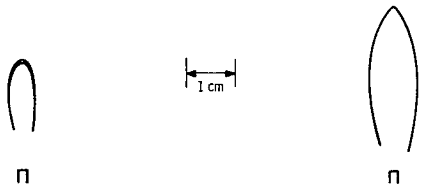

(a-1) Maximum flame radius R_{max} = 0.37 centimeter; normal gravity.

(a-2) Maximum flame radius R_{max} = 0.70 centimeter; zero gravity.

(a) Run 2.

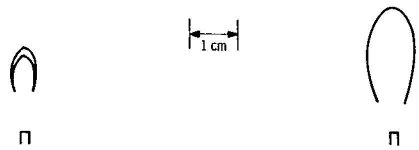

(b-1) Maximum flame radius R_{max} = 0.37 centimeter; normal gravity.

(b-2) Maximum flame radius R_{max} = 0.72 centimeter; zero gravity.

(b) Run 3.

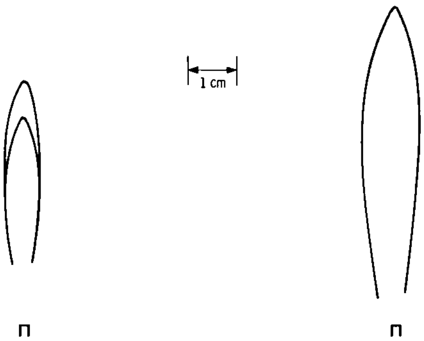

(c-1) Maximum flame radius R_{max} = 0.51 centimeter; normal gravity.

(c-2) Maximum flame radius R_{max} = 0.83 centimeter; zero gravity.

(c) Run 4.

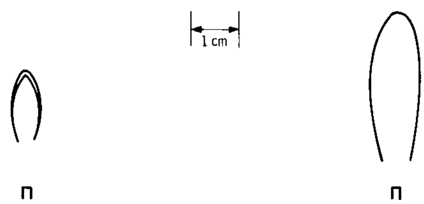

(d-1) Maximum flame radius R_{max} = 0.42 centimeter; normal gravity.

(d-2) Maximum flame radius R_{max} = 0.74 centimeter; zero gravity.

(d) Run 5.

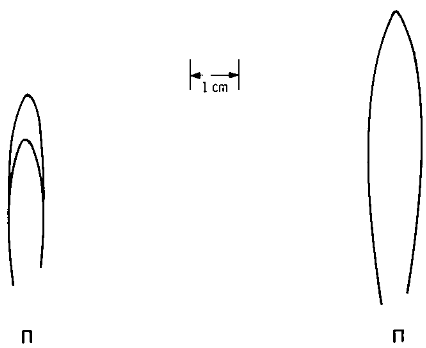

(e-1) Maximum flame radius R_{max} = 0.51 centimeter; normal gravity.

(e-2) Maximum flame radius R_{max} = 0.78 centimeter; zero gravity.

(e) Run 6.

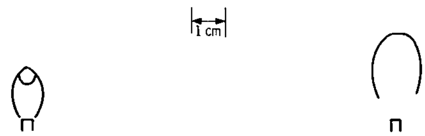

(f-1) Maximum flame radius R_{max} = 0.32 centimeter; normal gravity.

(f-2) Maximum flame radius R_{max} = 0.48 centimeter; zero gravity.

(f) Run 8.

Figure 13. - Steady-state flame geometry in normal and zero gravity.

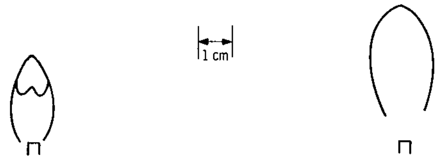

(g-1) Maximum flame radius R_{max} = 0.44 centimeter; normal gravity.

(g-2) Maximum flame radius R_{max} = 0.60 centimeter; zero gravity.

(g) Run 9.

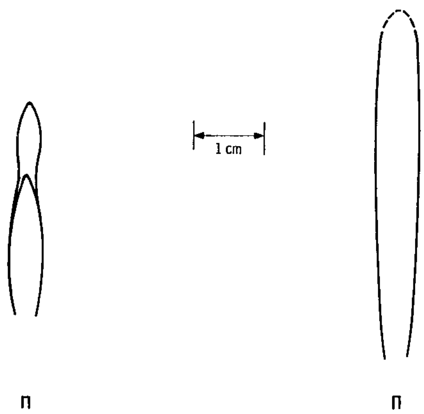

(h-1) Maximum flame radius R_{max} = 0.63 centimeter; normal gravity.

(h-2) Maximum flame radius R_{max} = 0.91 centimeter; zero gravity.

(h) Run 23.

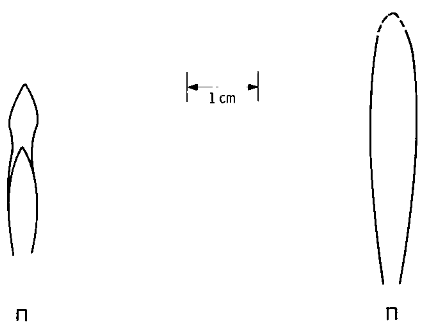

(i-1) Maximum flame radius R_{max} = 0.58 centimeter; normal gravity.

(i-2) Maximum flame radius R_{max} = 0.95 centimeter; zero gravity.

(i) Run 24.

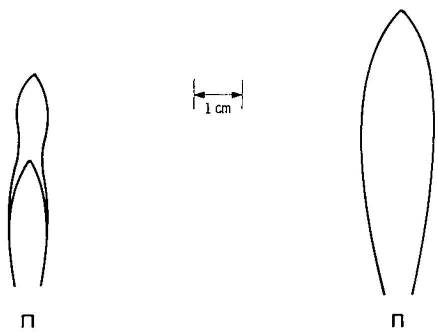

(j-1) Maximum flame radius R_{max} = 0.58 centimeter; normal gravity.

(j-2) Maximum flame radius R_{max} = 1.04 centimeters; zero gravity.

(j) Run 25.

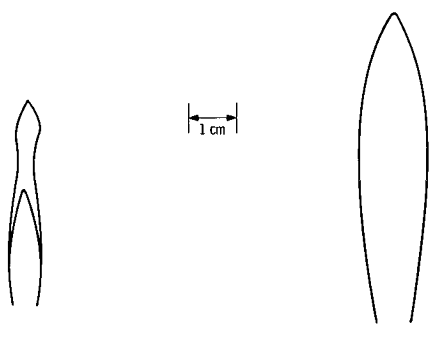

(k-1) Maximum flame radius R_{max} = 0.48 centimeter; normal gravity.

(k-2) Maximum flame radius R_{max} = 0.92 centimeter; zero gravity.

(k) Run 30.

Figure 13. - Concluded.

A flame, by definition, is determined by the positioning of a chemical reaction not by the observed radiation in its vicinity. This is particularly true for flames observed on film because of the dependence of the recorded image on parameters such as film type, camera speed, camera lens, and film processing. In normal gravity, defining the reaction zone shape coincident with the extent of the observed radiation is probably quite accurate because of the thinness of the reaction zone and the high temperature gradients. However, in zero gravity, the possibility exists that the reaction zone is relatively thick (ref. 11). This is supported in the present work by the observed changes in color through the zero-gravity flames from yellow in the center to orange at its extremities. Therefore, the zero-gravity shapes presented in figure 13 should only be considered as a good approximation to the outer extent of the flame position.

Flame existence in zero gravity. - One of the goals of this investigation, as an extension of the work reported in reference 1, was to determine those conditions for which steady state flames existed in zero gravity. Accordingly, it was decided to systematically vary the gas jet Reynolds number to determine if that parameter correlated flame existence. Table II presents the data in terms of the zero-gravity flame condition (extinguished, transient, or steady state) as a function of burner size and gas jet Reynolds number. The data from reference 1 is included in the table. For each burner size, the data is arranged in ascending order of Reynolds number. For the smaller burners, the flames generally progressed from an extinguished to a transient to a steady state condition as the Reynolds number increased. As burner size increased, first the steady state and then the transient condition disappeared so that only the extinguished condition resulted.

In discussing the behavior of diffusion flames in zero gravity, it must be kept in mind that the data obtained from drop towers involve some transient effects. Certainly one would expect a certain amount of time to be required for the flame to react to a sudden change in gravity level. It is possible that the observed extinguishment is a result of transient fluid dynamic effects. In fact, there is some evidence in the transient flame data herein to suggest this. However, it is also possible that under certain circumstances diffusion flames ignited in zero gravity cannot exist in steady state. Bonne predicts in reference 4 that diffusion flames ignited in zero gravity naturally extinguish due to excessive radiative losses. Another potential extinguishment mechanism is the blanketing of the flame by the products of combustion which are not being removed at a fast enough rate because of the absence of buoyancy. Due to this lack of understanding, the data of table II must only be considered a conservative estimate of the conditions for which steady state flames exist in zero gravity.

TABLE II. - ZERO-GRAVITY FLAME CONDITIONS

Burner radius, R_o, cm	Run	Gas jet Reynolds number, Re_F	Condition
0.051	7	28.4	Extinguished
	8	40.9	Steady state
	9	60.6	
	3	79.5	
	2	106.0	
	5	109.8	
	6	185.6	
	4	195.0	
	1	251.8	(a)
0.0825	28	23.4	Extinguished
	29	35.1	Transient
	27	46.8	Transient
	26	67.9	Transient
	25	106.5	Steady state
	30	128.8	
	24	150.3	
	23	200.2	
0.113	10	17.1	Extinguished
	13	18.5	
	14	20.1	
	11	29.1	
	15	29.4	
	12	33.8	Transient
	16	36.9	Extinguished
	18	66.7	
	19	73.5	
	20	82.9	
	17	84.6	Transient
	21	165.0	Transient
	22	208.5	(a)
0.186	Ref. 1	12.9 to 54.1	Extinguished
0.318	Ref. 1	9.3 to 29.8	Extinguished
0.442	Ref. 1	6.5 to 17.9	Extinguished

[a]Out of camera field of view.

SUMMARY OF RESULTS

An experimental program was conducted to investigate gravity effects on laminar gas jet diffusion flames. The tests were conducted in a drop tower which made available 2.2 seconds of zero-gravity time. Motion-picture photographs were taken of a methane jet burning in quiescent air for various flow rates and burner sizes. The following results were obtained:

1. Steady state flames existed in zero gravity.

2. The geometry of steady state flames in zero gravity is significantly different than normal-gravity flames for the same flow rate and burner size. Methane-air flames were approximately 50 percent longer and wider in zero gravity than in normal gravity.

3. The colors of the visible radiation given off by the flames suggest that the zero-gravity flames (mostly orange) may be cooler than those in normal gravity (yellow and blue).

4. The dimensionless zero-gravity flame length (referenced to burner radius) was a linear function of the gas jet Reynolds number.

5. Steady state flames in zero gravity generally were more stable than those in normal gravity; that is, they did not oscillate as much.

6. The behavior of the flames (extinguished, transient, or steady state) in zero gravity was a function of burner size and gas jet Reynolds number.

Lewis Research Center,
National Aeronautics and Space Administration,
Cleveland, Ohio, October 15, 1971,
111-05.

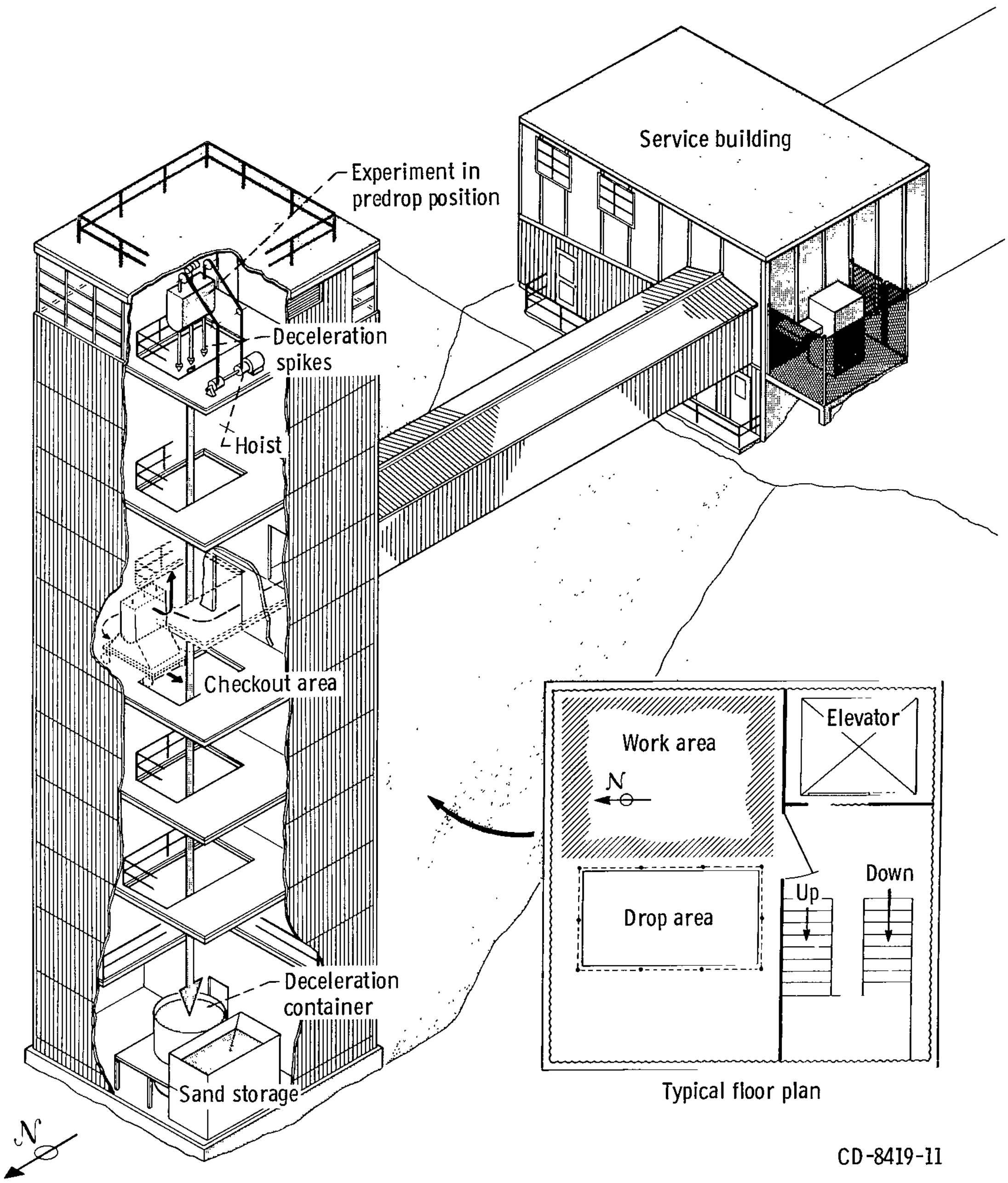

Figure 14. - 2.2-Second Zero Gravity Facility.

APPENDIX - APPARATUS AND PROCEDURE

Test Facility

The experimental data for this study were obtained in the Lewis Research Center's 2.2-Second Zero-Gravity Facility. A schematic diagram of this facility is shown in figure 14. The facility consists of a building 6.4 meters (21 ft) square by 30.5 meters (100 ft) tall. Contained within the building is a drop area 27 meters (89 ft) long with a cross section of 1.5 by 2.75 meters (5 by 9 ft).

Mode of operation. - A 2.2-second period of weightlessness was obtained by allowing the experiment package to free fall from the top of the drop area. In order to minimize drag on the experiment package, it was enclosed in a drag shield, designed with a high ratio of weight to frontal area and a low drag coefficient. The relative motion of the experiment package with respect to the drag shield during a test is shown in figure 15. Throughout the test the experiment package and drag shield fell freely and independently of each other; that is, no guide wires, electrical lines, and so forth were connected to either. Therefore, the only force acting on the freely falling experiment package was the air drag associated with the relative motion of the package within the enclosure of the

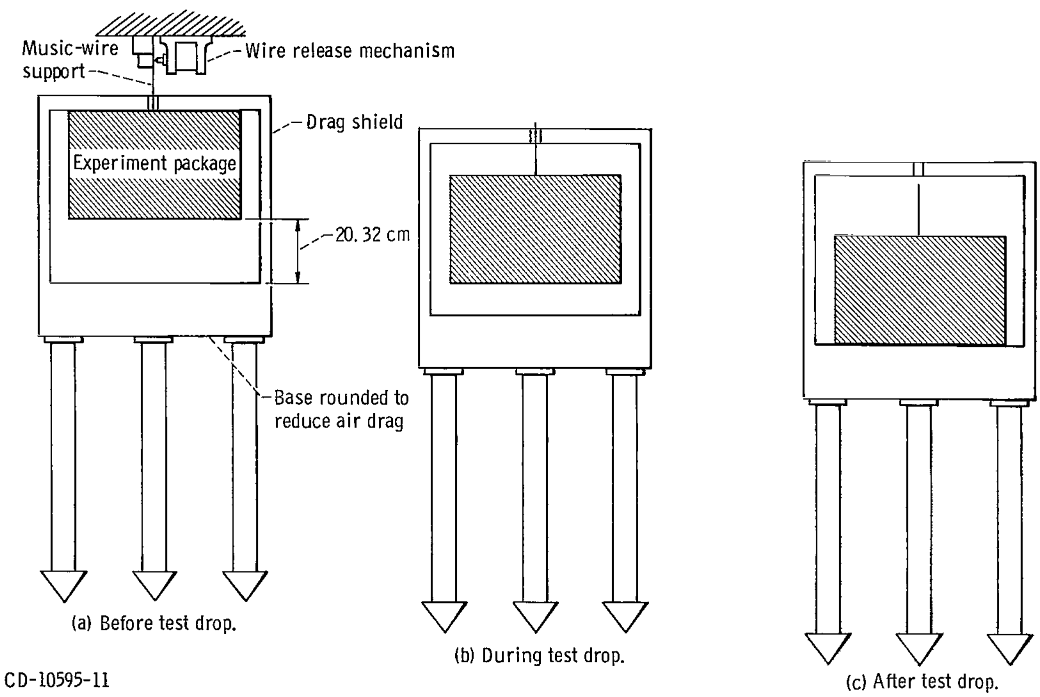

Figure 15. - Position of experiment package and drag shield before, during, and after test drop.

drag shield. This air drag resulted in an equivalent gravitational acceleration acting on the experiment, which is estimated to be below 10^{-5} g's.

Release system. - The experiment package, installed within the drag shield was suspended at the top of the drop area by a highly stressed music wire which was attached to the release system. This release system consisted of a double-acting air cylinder with a hard steel knife attached to the piston. Pressurization of the air cylinder drove the knife edge against the wire which was backed by an anvil. The resulting notch caused the wire to fail, smoothly releasing the experiment. No measurable disturbances were imparted to the package by this release procedure.

Recovery system. - After the experiment package and drag shield traversed the total length of the drop area, they were recovered after decelerating in a 2.2-meter (7-ft) deep container filled with sand. The deceleration rate (averaging 15 g's) was controlled by selectively varying the tips of the deceleration spikes mounted on the bottom of the drag shield (fig. 15). At the time of impact of the drag shield in the decelerator container, the experiment package traversed the vertical distance within the drag shield (compare figs. 15(a) and (c)).

Experimental Package

The experimental package, as shown in figure 16, contained a combustion chamber, camera, clock, methane flow system, carbon dioxide flow system, and associated controls and dc power supplies.

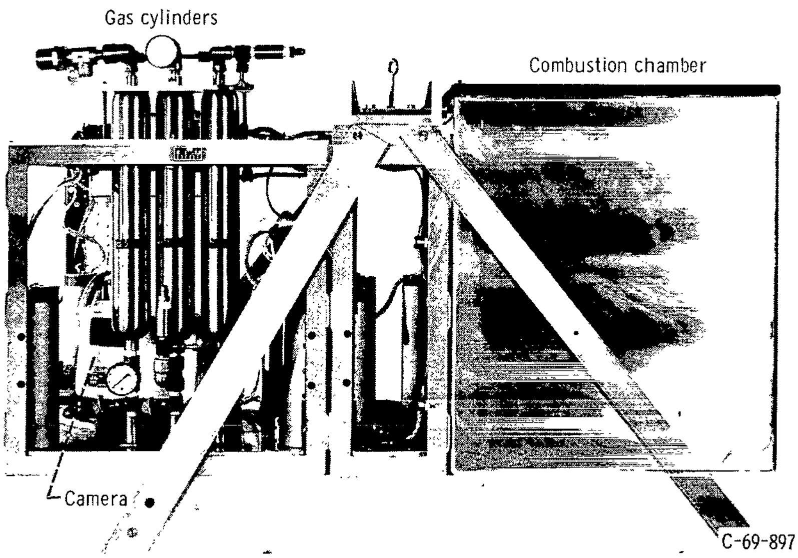

Figure 16. - Experiment package.

The combustion chamber contained the burner, lighting equipment, carbon dioxide inlets, and the ignition system. The burner extended approximately 2 centimeters above the floor and was positioned at the center of the chamber. The dimensions of the chamber were approximately 41 centimeters long by 41 centimeters wide by 48 centimeters high. The top of the chamber had holes in it to ensure equilization of pressure with the atmosphere during burning. The volume of the chamber was such that there was over 60 times the amount of air necessary to burn the fuel at the highest flow rate for at least 10 seconds. The igniter was a coiled 0.33-centimeter-diameter nichrome wire attached at its ends to copper rods. Current to the wire was supplied by a 14.4-volt, 1.75-ampere-hour pack of batteries. One wall of the chamber was a plastic sheet. Lighting was indirect so that the flames could be photographed against a black background.

The type of film used was color high-speed 16-millimeter Echtachrome EF (tungsten) manufactured by the Eastman Kodak Company. In order to maximize detail in the pictures, three lenses were used depending on the size of the flame. The aperature settings for the 17-, 25-, and 36-millimeter lenses were f-2.8, f-1.4, and f-1.1, respectively. The average film speed was approximately 400 frames per second, and it was processed to an ASA of 250.

The methane flow system included a 500-cubic-centimeter stainless-steel vessel, flow valves, a relief valve, a low-flow needle valve, two explosion-proof solenoids, stainless-steel tubing, and a pressure regulator. In this system, the solenoids were connected in series to ensure that flow stopped upon deactivation.

Carbon dioxide was included to dilute the contents of the combustion chamber below the flammability limit after the test. This system consisted of two 500-cubic-centimeter stainless-steel vessels, flow valves, a relief valve, two explosion-proof solenoids, and stainless-steel tubing. Mounting of the solenoids in parallel ensured flow upon activation.

Test Procedure

Calibrations. - Prior to the normal- and zero-gravity experimentation, calibrations to determine flame length as a function of flow rate were conducted, The flow measuring device, a rotameter, was installed in the methane flow system. Motion pictures were then taken of flames at different lengths, and the respective flow rates were recorded. Data were obtained for each of the different burners over the range of flow to be used in the experiments.

Experimentation. - The methane cylinder was charged to a pressure of approximately 14×10^5 newtons per square meter ($\cong$200 psi) and the carbon dioxide cylinders to about 34.5×10^5 newtons per square meter ($\cong$500 psi). The experiment package was placed in the drag shield and raised to the top of the tower.

Approximately 5 seconds before the drop, the lights were turned on, and the methane flow, camera, and clock were started. One second later, the ignition system was activated. The remaining 4 seconds before the drop were used to permit the flame to come to steady state. The drag shield and experiment were released, and about 2 seconds of zero-gravity data were obtained. Just before impact in the sand, the methane flow was stopped, the camera, clock, and lights were turned off, and the carbon dioxide system was activated. These steps removed potential ignition sources and diluted a possible combustible mixture.

NASA-Langley, 1972 —— 33 E-6570

NATIONAL AERONAUTICS AND SPACE ADMISTRATION
WASHINGTON, D.C. 20546

OFFICIAL BUSINESS
PENALTY FOR PRIVATE USE $300

FIRST CLASS MAIL

POSTAGE AND FEES PAID
NATIONAL AERONAUTICS AND
SPACE ADMINISTRATION

U.S.MAIL

014 001 C1 U 33 711217 S00903DS
DEPT OF THE AIR FORCE
AF WEAPONS LAB (AFSC)
TECH LIBRARY/WLOL/
ATTN: E LOU BOWMAN, CHIEF
KIRTLAND AFB NM 87117

POSTMASTER: If Undeliverable (Section 158 Postal Manual) Do Not Return

"The aeronautical and space activities of the United States shall be conducted so as to contribute . . . to the expansion of human knowledge of phenomena in the atmosphere and space. The Administration shall provide for the widest practicable and appropriate dissemination of information concerning its activities and the results thereof."

—NATIONAL AERONAUTICS AND SPACE ACT OF 1958

NASA SCIENTIFIC AND TECHNICAL PUBLICATIONS

TECHNICAL REPORTS: Scientific and technical information considered important, complete, and a lasting contribution to existing knowledge.

TECHNICAL NOTES: Information less broad in scope but nevertheless of importance as a contribution to existing knowledge.

TECHNICAL MEMORANDUMS: Information receiving limited distribution because of preliminary data, security classification, or other reasons.

CONTRACTOR REPORTS: Scientific and technical information generated under a NASA contract or grant and considered an important contribution to existing knowledge.

TECHNICAL TRANSLATIONS: Information published in a foreign language considered to merit NASA distribution in English.

SPECIAL PUBLICATIONS: Information derived from or of value to NASA activities. Publications include conference proceedings, monographs, data compilations, handbooks, sourcebooks, and special bibliographies.

TECHNOLOGY UTILIZATION PUBLICATIONS: Information on technology used by NASA that may be of particular interest in commercial and other non-aerospace applications. Publications include Tech Briefs, Technology Utilization Reports and Technology Surveys.

Details on the availability of these publications may be obtained from:

SCIENTIFIC AND TECHNICAL INFORMATION OFFICE

NATIONAL AERONAUTICS AND SPACE ADMINISTRATION

Washington, D.C. 20546